Convergence of vector spherical wave expansion method applied to near-field radiative transfer

Karthik Sasihithlu and Arvind Narayanaswamy*
Department of Mechanical Engineering, Columbia University, New York, New York 10027, USA
**arvind.narayanaswamy@columbia.edu*

Abstract: Near-field radiative transfer between two objects can be computed using Rytov's theory of fluctuational electrodynamics in which the strength of electromagnetic sources is related to temperature through the fluctuation-dissipation theorem, and the resultant energy transfer is described using the dyadic Green's function of the vector Helmholtz equation. When the two objects are spheres, the dyadic Green's function can be expanded in a series of vector spherical waves. Based on comparison with the convergence criterion for the case of radiative transfer between two parallel surfaces, we derive a relation for the number of vector spherical waves required for convergence in the case of radiative transfer between two spheres. We show that when electromagnetic surface waves are active at a frequency the number of vector spherical waves required for convergence is proportional to R_{max}/d when $d/R_{max} \to 0$, where R_{max} is the radius of the larger sphere, and d is the smallest gap between the two spheres. This criterion for convergence applies equally well to other near-field electromagnetic scattering problems.

OCIS codes: (240.6690) Surface waves; (290.4020) Mie theory; (290.4210) Multiple scattering; (290.6815) Thermal emission; (260.2160) Energy transfer; (030.5620) Radiative transfer.

References and links

1. G. Mie, "Contributions on the optics of turbid media, particularly colloidal metal solutions" Tech. Rep. SAND78-6018, Translated by P. Newman, Sandia Labs (1978), (an english translation of G. Mie's 1908 paper.).
2. J. H. Bruning and Y. Lo, "Multiple scattering by spheres" Tech. Rep. Antenna Laboratory Report No. 69-5, University of Illinois, Urbana, Illinois (1969).
3. J. H. Bruning and Y. T. Lo, "Multiple scattering of EM waves by spheres Part I–multipole expansion and ray-optical solutions" IEEE Trans. Antenn. Propag. **AP-19**, 378–390 (1971).
4. C. Liang and Y. T. Lo, "Scattering by two spheres," Radio Sci. **2**, 1481 (1967).
5. R. Crane, "Cooperative scattering by dielectric spheres," Tech. Rep., Lincoln Laboratory, M.I.T, Lexington, MA (1967).
6. E. Merzbacher, *Quantum Mechanics* (Wiley, 1997).
7. S. Stein, "Addition theorems for spherical wave functions," Q. Appl. Math. **19**, 15–24 (1961).
8. O. Cruzan, "Translational addition theorems for spherical vector wave functions," Q. Appl. Math. **20**, 33–40 (1962).
9. M. Kerker, *The Scattering of Light and Other Electromagnetic Radiation* (Academic,1969).
10. D. W. Mackowski, "Electrostatics analysis of radiative absorption by sphere clusters in the Rayleigh limit: application to soot particles." Appl. Opt. **34**, 3535–3545 (1995).
11. H. Kimura, L. Kolokolova, and I. Mann, "Light scattering by cometary dust numerically simulated with aggregate particles consisting of identical spheres," Astron. Astrophys. **449**, 1243–1254 (2006).

#147197 - $15.00 USD Received 9 May 2011; revised 26 May 2011; accepted 27 May 2011; published 6 Jun 2011

12. P. L. Stiles, J. A. Dieringer, N. C. Shah, and R. P. Van Duyne, "Surface-enhanced Raman spectroscopy." Annu. Rev. Anal. Chem. **1**, 601–626 (2008).
13. A. Campion and P. Kambhampati, "Surface-enhanced Raman scattering," Chem. Soc. Rev. **27**, 241 (1998).
14. D. W. Pohl, W. Denk, and M. Lanz, "Optical stethoscopy: Image recording with resolution $\lambda/20$," Appl. Phys. Lett. **44**, 651–653 (1984).
15. U. Durig, D. W. Pohl, and F. Rohner, "Near-field optical-scanning microscopy," J. Appl. Phys. **59**, 3318–3327 (1986).
16. W. L. Barnes, A. Dereux, and T. W. Ebbesen, "Surface plasmon subwavelength optics." Nature **424**, 824–830 (2003).
17. A. Zayats, I. Smolyaninov, and A. Maradudin, "Nano-optics of surface plasmon polaritons," Phys. Rep. **408**, 131–314 (2005).
18. S. Kawata, Y. Inouye, and P. Verma, "Plasmonics for near-field nano-imaging and superlensing," Nat. Photonics **3**, 388–394 (2009).
19. K. Joulain, J.-P. Mulet, F. Marquier, R. Carminati, and J.-J. Greffet, "Surface electromagnetic waves thermally excited: Radiative heat transfer, coherence properties and Casimir forces revisited in the near field," Surf. Sci. Rep. **57**, 59–112 (2005).
20. M. Francoeur and M. P. Menguc, "Role of fluctuational electrodynamics in near-field radiative heat transfer," J. Quant. Spectrosc. Radiat. Transfer **109**, 280–293 (2008).
21. Y. De Wilde, F. Formanek, R. Carminati, B. Gralak, P. Lemoine, K. Joulain, J. Mulet, Y. Chen, and J. Greffet, "Thermal radiation scanning tunnelling microscopy," Nature **444**, 740–743 (2006).
22. A. Kittel, U. Wischnath, J. Welker, O. Huth, F. Ruting, and S. Biehs, "Near-field thermal imaging of nanostructured surfaces," Appl. Phys. Lett. **93**, 193109 (2008).
23. D. Polder and M. Van Hove, "Theory of radiative heat transfer between closely spaced bodies," Phys. Rev. B **4**, 3303–3314 (1971).
24. J.-P. Mulet, K. Joulain, R. Carminati, and J.-J. Greffet, "Enhanced radiative transfer at nanometric distances," Microscale Thermo. Eng. **6**, 209–222 (2002).
25. J. B. Pendry, "Radiative exchange of heat between nanostructures," J. Phys.: Condens. Matter **11**, 6621–6633 (1999).
26. M. Francoeur, M. Menguc, and R. Vaillon, "Near-field radiative heat transfer enhancement via surface phonon polaritons coupling in thin films," Appl. Phys. Lett. **93**, 043109 (2008).
27. A. Narayanaswamy, S. Shen, and G. Chen, "Near–field radiative heat transfer between a sphere and a substrate," Phys. Rev. B **78**, 115303 (2008).
28. S. Shen, A. Narayanaswamy, and G. Chen, "Surface phonon polaritons mediated energy transfer between nanoscale gaps," Nano Lett. **9**, 2909–2913 (2009).
29. A. Narayanaswamy, S. Shen, L. Hu, X. Chen, and G. Chen, "Breakdown of the planck blackbody radiation law at nanoscale breakdown of the planck blackbody radiation law at nanoscale gaps," Appl. Phys. A **96**, 357–362 (2009).
30. E. Rousseau, A. Siria, G. Jourdan, S. Volz, F. Comin, J. Chevrier, and J.-J. Greffet, "Radiative heat transfer at the nanoscale," Nat. Photonics **3**, 514–517 (2009).
31. S. Biehs, E. Rousseau, and J. Greffet, "Mesoscopic description of radiative heat transfer at the nanoscale," Phys. Rev. Lett. **105**, 234301 (2010).
32. P. Ben-Abdallah and K. Joulain, "Fundamental limits for noncontact transfers between two bodies," Phys. Rev. B **82**, 121419 (2010).
33. A. Narayanaswamy and G. Chen, "Surface modes for near field thermophotovoltaics," Appl. Phys. Lett. **82**, 3544–3546 (2003).
34. S. Basu, Z. Zhang, and C. Fu, "Review of near-field thermal radiation and its application to energy conversion," Int. J. Energy Res. **33**, 1203–1232 (2009).
35. M. Laroche, R. Carminati, and J.-J. Greffet, "Near-field thermophotovoltaic energy conversion," J. of Appl. Phys. **100**, 063704 (2006).
36. R. Yang, A. Narayanaswamy, and G. Chen, "Surface-plasmon coupled nonequilibrium thermoelectric refrigerators and power generators," J. Comput. Theor. Nanos. **2**, 75–87 (2005).
37. C. Otey and S. Fan, "Exact microscopic theory of electromagnetic heat transfer between a dielectric sphere and plate," Arxiv preprint arXiv:1103.2668(2011).
38. C. Hargreaves, "Radiative transfer between closely spaced bodies," Philips Res. Rep. Suppl. **5**, 1–80 (1973).
39. L. Hu, A. Narayanaswamy, X. Chen, and G. Chen, "Near-field thermal radiation between two closely spaced glass plates exceeding plancks blackbody radiation law," Appl. Phys. Lett. **92**, 133106 (2008).
40. R. Ottens, V. Quetschke, S. Wise, A. Alemi, R. Lundock, G. Mueller, D. Reitze, D. Tanner, and B. Whiting, "Near-field radiative heat transfer between macroscopic planar surfaces," Arxiv preprint arXiv:1103.2389 (2011).
41. A. Narayanaswamy and G. Chen, "Thermal near–field radiative transfer between two spheres," Phys. Rev. B **77**, 075125 (2008).
42. J. D. Jackson, *Classical Electrodynamics* (John Wiley, 1998).
43. J. Stratton, *Electromagnetic Theory* (Wiley-IEEE Press, 2007).

#147197 - $15.00 USD Received 9 May 2011; revised 26 May 2011; accepted 27 May 2011; published 6 Jun 2011

44. C. F. Bohren and D. R. Huffman, *Absorption and Scattering of Light by Small Particles* (Wiley-Interscience, 1998).
45. W. C. Chew, *Waves and Fields in Inhomogeneous Media* (IEEE Press, 1995).
46. W. C. Chew, "Efficient ways to compute the vector addition theorem," J. Electromagn. Wave **7**, 651–665 (1993).
47. W. C. Chew, "Derivation of the vector addition theorem," Microw. Opt. Technol. Let. **3**, 256–260 (1990).
48. W. Wiscombe, "Mie scattering calculations: advances in technique and fast, vector-speed computer codes," Tech. rep., NCAR/TN-140+ STR, National Center for Atmospheric Research, Boulder, Colorado (1996).
49. W. Chew, E. Michielssen, J. Song, and J. Jin, *Fast and efficient algorithms in computational electromagnetics*, (Artech House, Inc., 2001).
50. N. A. Gumerov and R. Duraiswami, "Computation of scattering from n spheres using multipole reexpansion," J. Acoust. Soc. Am. **112**, 2688–2701 (2002).
51. M. Quinten, A. Pack, and R. Wannemacher, "Scattering and extinction of evanescent waves by small particles," Appl. Phys. B **68**, 87–92 (1999).
52. V. Yannopapas and N. Vitanov, "Spontaneous emission of a two-level atom placed within clusters of metallic nanoparticles," J. Phys.: Condens. Matter **19**, 096210 (2007).
53. W. Chew, "A derivation of the vector addition theorem," Microw. Opt. Technol. Let. **3**, 256–260 (1990).
54. A. Narayanaswamy and G. Chen, "Direct computation of thermal emission from nanostructures," *Annual Reviews of Heat Transfer* (Begell House, 2005), vol. **14**, pp. 169-195.

1. Introduction

Electromagnetic scattering from a sphere is a well studied topic since the seminal work of Mie [1]. The sphere is one of the few bodies for which the scattering behavior has been thoroughly investigated and hence can be used as an approximation to model interaction of electromagnetic radiation with particulate matter. Study of electromagnetic scattering from two spheres and in general from multiple spheres is equally important as it is necessary to understand the effect of multiple scattering from closely spaced particles. The first computationally viable solution to the problem of electromagnetic scattering by two spheres of arbitrary size was put forward by Bruning and Lo [2,3]. Prior works [4,5] involved the time consuming computation of Wigner's 3-j symbols [6] while applying the translational addition theorem introduced by Stein [7] and Cruzan [8]. Bruning and Lo overcame this problem by introducing an efficient recurrence relation to compute the translation coefficients.

In the analysis of scattering by spheres, depending on the location of the point at which the scattered electric and magnetic fields are calculated (or measured), *far-field* or *near-field* effects can dominate. For a sphere of radius R and excitation source of wavelength λ, near-field effects are dominant in regions that satisfy the condition $R \lesssim r \ll \lambda$. The far-field approximation is sufficient when (1) $r \gg R$, and (2) $r \gg \lambda$. Here r is the distance between the center of the sphere and the point at which the scattered fields are calculated. Some of the practical applications of mulitple sphere scattering, ranging from the study of scattering from aerosols [9] and soot particles [10] to applications like study of light scattering from comet dust [11], involve far-field phenomena – i.e., near-field effects are unimportant. The near-field response of a particle or surface to an electromagnetic excitation source is crucial in many applications, e.g. in surface enhanced Raman spectroscopy [12, 13], near-field scanning optical microscopy [14, 15], plasmonics and sub-wavelength optics [16–18], van der Waals and Casimir forces [19], near-field thermal radiative transfer [19, 20], and near-field thermal imaging [21, 22]. In particular, the near-field contribution to the thermal radiative transfer between polar dielectric surfaces (like SiO_2, SiC, etc) separated by a vacuum gap is dominated by tunneling of electromagnetic surface modes [23–25]. These modes are characterized by the presence of large energy density at the interface between the dielectric medium and vacuum and decay rapidly with distance from the surface [19].

Near-field effects lead to enhancement of thermal radiative transfer beyond the limits imposed by Planck's theory of thermal radiation [26–32] and can be exploited to increase the efficiency and power density of thermophotovoltaic [33–35] as well as thermoelectric energy

#147197 - $15.00 USD Received 9 May 2011; revised 26 May 2011; accepted 27 May 2011; published 6 Jun 2011

conversion devices [36]. Experimental confirmation of near-field enhancement of thermal radiation beyond Planck's limit has been possible by measuring radiative transfer between a microsphere and a flat surface [27, 28, 30, 37], and between two parallel surfaces [38–40]. However, with parallel surfaces, it has not been possible to explore near-field effects at sub-micron gaps. For this reason, numerical models of near-field radiative transfer between spherical surfaces are important. A method similar to the Mie theory, based on the vector spherical wave expansion, has been used to model such phenomena when spherical particles are involved [41]. We shall focus here on the numerical convergence of the vector spherical wave expansion method when near-field effects due to electromagnetic surface modes on the surface of a sphere are dominant. In particular, we will demonstrate the importance of a new convergence criteria by calculating the enhanced thermal radiative transfer between two silica spheres due to the tunneling of electromagnetic surface modes.

1.1. Vector spherical wave expansion

Let us consider the problem of scattering of an electromagnetic plane wave from a spherical particle in a homogeneous medium (vacuum) to give a brief introduction to the vector spherical wave expansion method that is used in this work. The origin of a spherical coordinate system, with respect to which the position vector $\boldsymbol{r} = (r, \theta, \phi)$ is defined, is located at the center of the sphere. The vector spherical waves, which are the fundamental solutions of the vector Helmholtz equation:

$$\boldsymbol{\nabla} \times \boldsymbol{\nabla} \times \boldsymbol{A}(\boldsymbol{r}) - k^2 \boldsymbol{A}(\boldsymbol{r}) = 0, \tag{1}$$

are given by:

$$\boldsymbol{M}_{lm}^{(p)}(k\boldsymbol{r}) \quad = \quad z_l^{(p)}(kr)\boldsymbol{V}_{lm}^{(2)}(\theta,\phi) \tag{2}$$

$$\boldsymbol{N}_{lm}^{(p)}(k\boldsymbol{r}) \quad = \quad \zeta_l^{(p)}(kr)\boldsymbol{V}_{lm}^{(3)}(\theta,\phi) + \frac{z_l^{(p)}(kr)}{kr}\sqrt{l(l+1)}\boldsymbol{V}_{lm}^{(1)}(\theta,\phi) \tag{3}$$

where $\boldsymbol{M}_{lm}^{(p)}(k\boldsymbol{r})$ and $\boldsymbol{N}_{lm}^{(p)}(k\boldsymbol{r})$ are vector spherical waves of order (l,m). l can take integer values from 0 to ∞. For each l, $|m| \leq l$. The superscript p refers to the radial behavior of the waves. For $p = 1$, the $\boldsymbol{M}$ and $\boldsymbol{N}$ waves are regular waves and remain finite at the origin and $z_l^{(1)}(kr)$ is the spherical bessel function of order l. For $p = 3$, the $\boldsymbol{M}$ and $\boldsymbol{N}$ waves are outgoing spherical waves that are singular at the origin and $z_l^{(3)}(kr)$ is the spherical Hankel function of the first kind of order l. The radial function $\zeta_l^{(p)}(x) = \frac{1}{x}\frac{d}{dx}\left(xz_l^{(p)}(x)\right)$. $\boldsymbol{V}_{lm}^{(1)}(\theta,\phi)$, $\boldsymbol{V}_{lm}^{(2)}(\theta,\phi)$, and $\boldsymbol{V}_{lm}^{(3)}(\theta,\phi)$ are vector spherical harmonics of order (l,m) and can be expressed in terms of the spherical harmonics $Y_{lm}(\theta,\phi)$ and their derivatives [41, 42].

The vector spherical waves $\boldsymbol{M}_{lm}^{(p)}(k\boldsymbol{r})$ and $\boldsymbol{N}_{lm}^{(p)}(k\boldsymbol{r})$ are related by $\boldsymbol{N}_{lm}^{(p)}(k\boldsymbol{r}) = \frac{1}{k}\boldsymbol{\nabla} \times \boldsymbol{M}_{lm}^{(p)}(k\boldsymbol{r})$ and $\boldsymbol{M}_{lm}^{(p)}(k\boldsymbol{r}) = \frac{1}{k}\boldsymbol{\nabla} \times \boldsymbol{N}_{lm}^{(p)}(k\boldsymbol{r})$. The completeness of the functions $\boldsymbol{M}_{lm}^{(p)}(k\boldsymbol{r})$ and $\boldsymbol{N}_{lm}^{(p)}(k\boldsymbol{r})$ allows the scattered electromagnetic field to be expanded in an infinite series as [43]:

$$\boldsymbol{E}(\boldsymbol{r}) = \sum_{l=1}^{\infty}\sum_{m=-l}^{l}\left(A_{lm}^{(p)}\boldsymbol{M}_{lm}^{(p)}(k\boldsymbol{r}) + B_{lm}^{(p)}\boldsymbol{N}_{lm}^{(p)}(k\boldsymbol{r})\right) \tag{4}$$

$$\boldsymbol{H}(\boldsymbol{r}) = \frac{ik}{\omega\mu}\sum_{l=1}^{\infty}\sum_{m=-l}^{l}\left(A_{lm}^{(p)}\boldsymbol{N}_{lm}^{(p)}(k\boldsymbol{r}) + B_{lm}^{(p)}\boldsymbol{M}_{lm}^{(p)}(k\boldsymbol{r})\right) \tag{5}$$

#147197 - $15.00 USD Received 9 May 2011; revised 26 May 2011; accepted 27 May 2011; published 6 Jun 2011

where $k^2(\boldsymbol{r}) = \omega^2 \varepsilon(\boldsymbol{r}) \mu(\boldsymbol{r})$. Here the dielectric permittivity, $\varepsilon(\boldsymbol{r})$, and magnetic permeability, $\mu(\boldsymbol{r})$, are frequency dependent piecewise constant functions with a discontinuity at the surface of the sphere. Since we are dealing with nonmagnetic materials, $\mu(\boldsymbol{r}) = 1$. For the interior of the sphere, we use $p = 1$ (regular vector spherical waves). For the exterior of the sphere, we use $p = 3$ (outgoing vector spherical waves). The excitation source can also be expanded in terms of the vector spherical waves. The coefficients $A_{lm}^{(p)}$ and $B_{lm}^{(p)}$ are obtained by satisfying the boundary conditions on the surface of the sphere. Subsequently, relevant quantities such as absorption and scattering cross-sections are obtained by appropriate combinations of $A_{lm}^{(3)}$ and $B_{lm}^{(3)}$ [44]. When multiple spheres are involved, boundary conditions have to be satisfied simultaneously on the surface of each of the spheres. This can be achieved by using the vector translation theorems that relate the vector spherical waves with respect to the center of one of the spheres to the vector spherical waves with respect to the center of another sphere [45–47].

1.2. Convergence criteria

Irrespective of single sphere or multiple sphere scattering, as a practical matter, the infinite series in Eq. (4) and Eq. (5) need to be truncated (in indices l and m), retaining only enough terms necessary to ensure a sufficiently accurate approximation. The number of terms to retain depends on different length scales pertinent to the problem. For far-field scattering by a single sphere, the relevant length scales are the radius of the sphere, R, and the wavelength of incident radiation, λ. The number of terms for convergence N_{conv} is given by [44, 48, 49]

$$N_{conv} = a + x + bx^{1/3} \tag{6}$$

where $x = 2\pi R/\lambda$, and a is 1 or 2 and b is 4 or 4.05, depending on x. These values of a and b are obtained empirically and the resulting expansion gives an error less than 0.01 %. For far-field scattering by two spheres shown in Fig. 1(a), the relevant length scales are the radii of spheres R_1 and R_2, the wavelength λ, and the center-to-center distance between the spheres, D. In this case, a different criterion has been proposed [50]

$$N_{conv} = e\pi \frac{D}{\lambda}, \tag{7}$$

where e is the base of natural logarithm. While the convergence criteria in Eq. (6) and (7) are relevant for far-field scattering, near-field effects lead to several peculiarities and hence we can expect different criteria for the number of terms of convergence. This is especially true when surface plasmon and/or phonon polaritons lead to enormous enhancement of the field amplitude near the interfaces. Hence for problems involving near-field effects the role of the gap d between the bodies can be expected to be prominent in deciding the number of terms for convergence.

The fact that scattering and absorption of evanescent waves lead to increased contributions from higher order terms has been recognized previously. While analyzing scattering and extinction by small particles, Quinten et al [51] noted the increase in the contributions from higher order modes for scattering and absorption by evanescent waves as compared to propagating waves. Yannopapas and Vitanov [52] noticed difficulty in attaining convergence while calculating local density of states (LDOS) near the surface of a metallic sphere. However an explicit form for the number of terms for convergence along the lines of Eq. (6) or (7) has not been proposed for near-field scattering. A brief mention of a convergence criteria was made by Narayanaswamy and Chen in their analysis of surface phonon polariton mediated near-field radiative transfer between two closely spaced spheres [41]. While a scaling form for the number of terms of convergence was proposed, a more detailed error analysis was not pursued. In this paper a comprehensive error analysis has been made for computation of near-field radiative

#147197 - $15.00 USD Received 9 May 2011; revised 26 May 2011; accepted 27 May 2011; published 6 Jun 2011

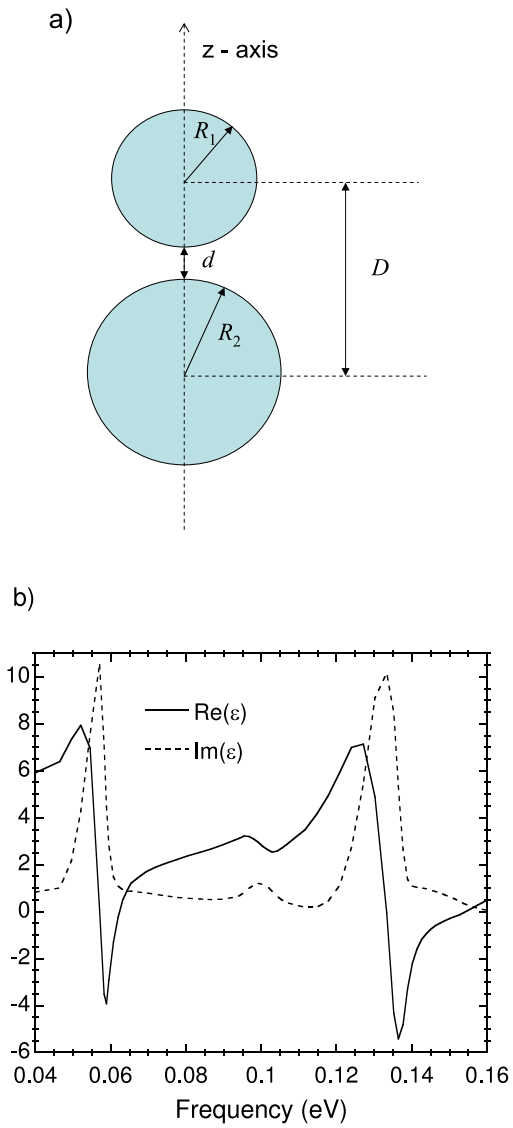

Fig. 1. **(a)** The configuration of two spheres for which the study is performed. **(b)** The variation of real and imaginary part of the dielectric function (ε) of silica in the frequency range under consideration.

transfer between two silica spheres of equal radii. Based on the error analysis we propose a criterion for the number of terms required to attain an error of less than 1% . We also extend this formulation for the case of two spheres of unequal radii.

2. Two sphere problem

Only a brief desription of the two sphere problem relevant to the topic of convergence of the vector spherical wave expansion method is discussed here. The configuration of two spheres which lie on the common z-axis and whose centers are separated by a distance D is shown in

#147197 - $15.00 USD Received 9 May 2011; revised 26 May 2011; accepted 27 May 2011; published 6 Jun 2011

Fig. 1(a). The symmetry in this configuration of the two spheres ensures that Eq. (4) and Eq. (5) can be simplified to be written as:

$$\boldsymbol{E}(\boldsymbol{r}) = \sum_{m=0}^{\infty}\sum_{l=(m,1)}^{\infty}(A_{lm}^{(p)}\boldsymbol{M}_{lm}^{(p)}(k\boldsymbol{r})+B_{lm}^{(p)}\boldsymbol{N}_{lm}^{(p)}(k\boldsymbol{r})) \quad (8)$$

$$\boldsymbol{H}(\boldsymbol{r}) = \frac{ik}{\omega\mu}\sum_{m=0}^{\infty}\sum_{l=(m,1)}^{\infty}(A_{lm}^{(p)}\boldsymbol{N}_{lm}^{(p)}(k\boldsymbol{r})+B_{lm}^{(p)}\boldsymbol{M}_{lm}^{(p)}(k\boldsymbol{r})), \quad (9)$$

where the symbol $(m,1)$ refers to the greater of m and 1. This step is more useful than the trivial simplification it appears to be. In Eq. (8) and (9), the computation for a given value of m is decoupled almost entirely from other values of m. The only link between computations for different values of m is that the recursive scheme for calculating vector translation coefficients at m requires the coefficients for $m-1$ and $m-2$ [53]. The quantity of interest in near-field radiative transfer is the linearized thermal conductance G (units WK^{-1}) between the two spheres. It is defined as:

$$G = \lim_{T_1\to T_2}\frac{Q(T_1,T_2)}{T_1-T_2}, \quad (10)$$

where $Q(T_1,T_2)$ is the rate of heat transfer between the two spheres at temperatures T_1 and T_2. Just as scattering or absorption coefficients can be used as metrics to gauge convergence for far-field radiation, we can similarly use conductance to gauge the convergence of scattering response in the near-field region. The heat transfer parameter G is related to the electromagnetic problem by expressing it in terms of the vector spherical expansion of the dyadic Green's function of the vector Helmholtz equation [41]. The expansion is similar to Eqs. (4) and (5) [43, 45]. Further details of the elctromagnetic formulation are available in Narayanaswamy and Chen [41]. The spheres are made of silica, the dielectric function of which is plotted as a function of frequency in Fig. 1(b). By observing the variation of the dielectric function with frequency it can be deduced that silica supports surface phonon-polaritons between 0.05-0.065 eV and 0.13-0.1405 eV. Hence computations are carried out in the frequency range 0.04-0.16 eV. In addition to conductance G, we also define a spectral conductance $G_\omega(\omega)$ that is related to G by the relation $G=\int G_\omega(\omega)\,d\omega$. The behavior of $G_\omega(\omega)$ is useful in showing the difference in convergence depending on whether or not surface phonon polaritons are active at that frequency. The numerical scheme itself proceeds along the following lines: (1) Choose a value of $l=N_{conv}$ to truncate the summation over l in Eq. (8) and Eq. (9). (2) Compute the electric and magnetic fields for each value of m, and from that the contribution to $G_\omega(\omega)$. This step is continued until the contribution from $m=M_{conv}$ has reached a sufficiently low value. (3) Repeat steps (1) and (2) for all frequencies to obtain G. Even though all values of m satisfying $|m|\le N_{conv}$ can contribute to the overall conductance, we will show that $M_{conv}\ll N_{conv}$ in practice.

2.1. Convergence of summation over l

To find the number of l terms required in Eq. (8) and Eq. (9) for convergence of near-field quantities for the two sphere problem, comparison is drawn with the well understood case of near-field transfer between two half-spaces [23, 24, 54]. In the latter case, the summations in Eq. (8) and Eq. (9) are replaced by integrals of the form $\int_0^\infty dk_{in}\,f(k_{in})\exp(-k_{in}z)$, where k_{in} is the in-plane wavevector, z is the spacing between the two half-spaces, and $f(k_{in})$ is an appropriately defined function. It is seen that only wavevectors satisfying the condition $k_{in}\lesssim 1/z$ contribute to the integral. The equivalent of the in-plane wavevector for a sphere is the wavelength of spatial variation of the field on the surface of the sphere. For $l=N_{conv}$, the

#147197 - $15.00 USD Received 9 May 2011; revised 26 May 2011; accepted 27 May 2011; published 6 Jun 2011

periodicity of the spatial variation is determined by the behavior of $Y_{N_{conv},m}$, $|m| \leq N_{conv}$. The smallest wavelength on the surface is given by $2\pi R/N_{conv}$, resulting in a maximum in-plane wavevector-equivalent of N_{conv}/R. By analogy with the convergence requirement for two half-spaces, we obtain $N_{conv}/R \sim 1/d$ or

$$N_{conv} = C\frac{R}{d}, \tag{11}$$

where C is a constant (or a weak function of R) that is dependent on the desired accuracy of the conductance. This criterion is sufficient for the analysis of radiative transfer between spheres of submicron radii where the radiative transfer is dominated by near-field effects. However, for spheres of larger radii where the contribution from propagating waves is not negligible, we have observed that the above criterion is not sufficient to attain convergence and the equation needs to be modified to :

$$N_{conv} = C\frac{R}{d} + e\pi\frac{D}{\lambda}, \tag{12}$$

with the additional term taken from Eq. (7).

In order to quantify the error due to retaining contributions only from wave functions with $l \leq N$ in Eq. (8) and Eq. (9), the conductance G and spectral conductance G_ω are plotted as a function of N in Fig. 2 and Fig. 3 respectively. It is seen that an exponentially decaying function of the form $G(N) = G_\infty + ae^{-bN}$ matches the variation of G (and G_ω) adequately, where G_∞ denotes the value of G as $N \to \infty$, and a and b are constants. The relative error $E(N)$ (in %) for total conductance, defined as $E(N) = (G(N) - G_\infty)/G_\infty$, is also plotted in Fig. 2. The conductance $G(N)$ and error $E(N)$ for $R = 10\ \mu$m and $R = 25\ \mu$m, with $d/R = 0.01$, are shown in Fig. 2(a) and 2(b) respectively. The difference between the convergence of the numerical method at nonresonant (0.1005 eV) and resonant (0.061 eV) frequencies is illustrated by plotting the spectral conductance for $R = 10\ \mu$m and $d/R = 0.01$ as a function of N in Fig. 3(a) and Fig. 3(b). Also plotted are the relative errors in spectral conductance at these frequencies.

The exponential decay in the error values is observed for both these frequencies. As expected, convergence to a given relative error requires a larger value of N at a resonant frequency than at a non-resonant frequency. For instance, at $N = 2R/d$ the relative error for the resonant frequency is ≈ 3 % while it is ≈ 0.2 % at the non-resonant frequency.

While Eq. (12) proposes a scaling form for N_{conv}, the constant C needs to be quantified for attaining a given relative error. This can be obtained by analyzing the variation of N_{conv} with R/d for spheres of different radii. Figure 4 shows the dependence of N_{conv} to attain 1 % error on R/d for spheres of both submicron radii and larger radii at the resonant frequency (0.061 eV). It is apparent that C assumes a constant value (≈ 2.72) at the resonant frequency. For total conductance, $C = 2$ is sufficient to attain 1% error as seen in Fig. 2. It should be noted that these values of C are particular to the case of radiative transfer between silica spheres. This constant is expected to vary weakly with the dielectric properties of the material(s) of the spheres. However the scaling form shown in Eq. (11) was proposed without taking into consideration the material of the spheres and hence can be used for any material that supports surface phonon or plasmon polaritons.

For the sake of completion we have also analyzed the convergence of conductance between spheres of unequal radii. For two spheres of radii R_1 and R_2 with $R_1 < R_2$, N_{conv} can be expected to scale with R_2 as:

$$N_{conv} = C\frac{R_2}{d} + e\pi\frac{D}{\lambda}, \tag{13}$$

The variation of spectral conductance G_ω as a function of N for two spheres with $R_1 = 2\,\mu$m, $R_2 = 40\,\mu$m and $d = 200$ nm at a nonresonant frequency (0.1005 eV) and a resonant frequency (0.061 eV) are shown in Fig. 5(a) and Fig. 5(b) respectively. Due to computational constraints

#147197 - $15.00 USD Received 9 May 2011; revised 26 May 2011; accepted 27 May 2011; published 6 Jun 2011

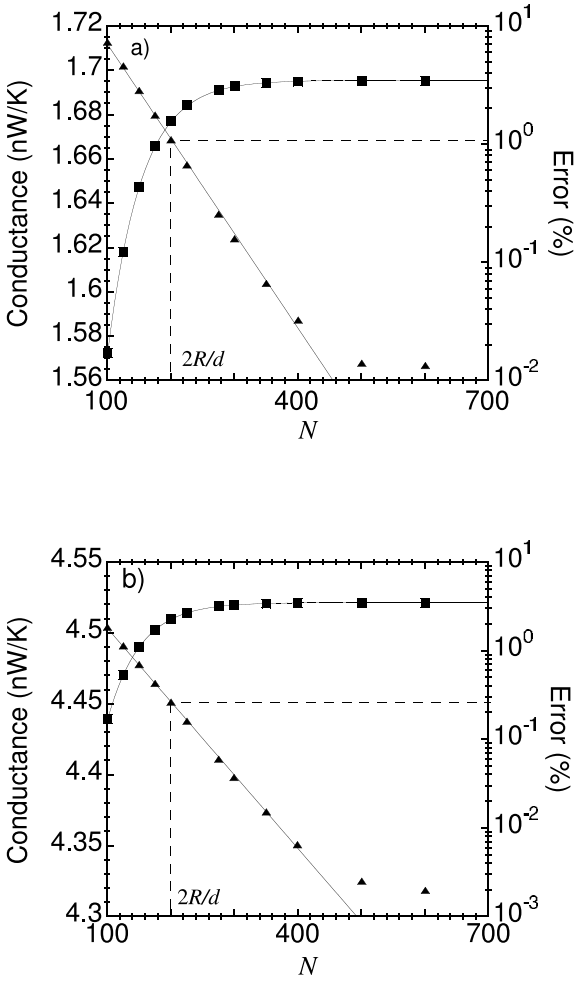

Fig. 2. Convergence of conductance (on the left axis) and error (on the right axis) shown for **(a)** $R = 10\,\mu$m spheres at d = 100 nm and **(b)** $R = 25\,\mu$m spheres at d = 250 nm. The solid line through the relative error data points is included to illustrate the exponentially decaying trend.

#147197 - $15.00 USD Received 9 May 2011; revised 26 May 2011; accepted 27 May 2011; published 6 Jun 2011

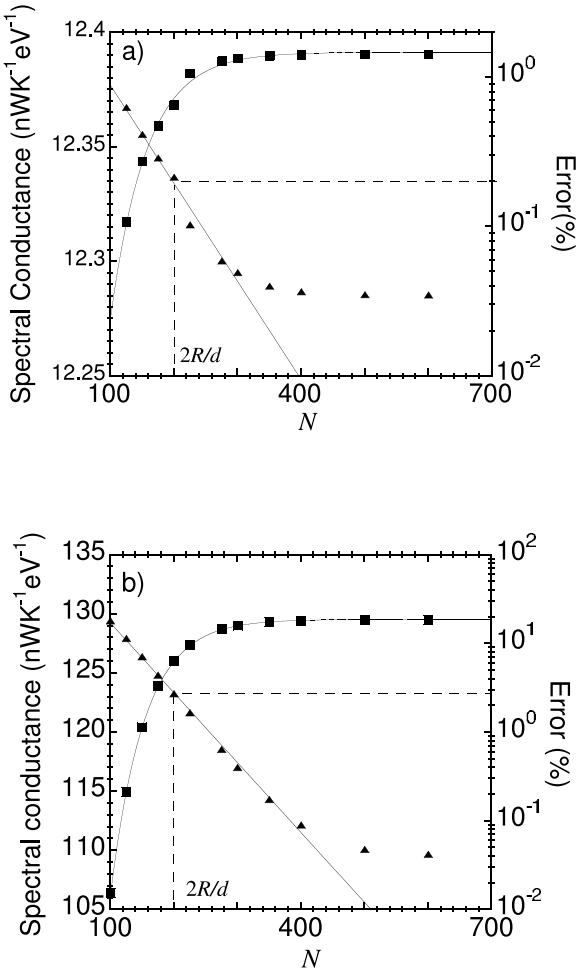

Fig. 3. Convergence of spectral conductance (on the left axis) and error (on the right axis) shown for $R = 10\,\mu$m spheres for d = 100 nm at **(a)** a nonresonant frequency (0.1005 eV) and **(b)** a resonant frequency (0.061 eV).

#147197 - $15.00 USD Received 9 May 2011; revised 26 May 2011; accepted 27 May 2011; published 6 Jun 2011

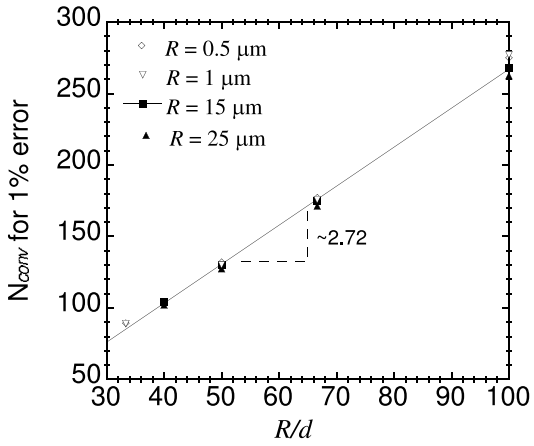

Fig. 4. Variation of N_{conv} with R/d for two equal-sized spheres with R = 500 nm, 1 μm, 15 μm and 25 μm.

the maximum number of terms considered for this study has been limited to $N = 3R_2/d$. From Fig. 5(b) we note that at the resonant frequency the value of constant C in Eq. (13), for 1% error, turns out approximately to be the same as the value obtained for equal radii [see Fig. 3(b)]. Hence we conclude that Eq. (13) is expected to hold true even in the limiting case of $R_1 \to 0$, which implies that to determine the scattered field due to excitation by a dipole current source at a distance $z(\ll \lambda)$ from the surface of a sphere of radius R, N_{conv} scales as R/z. This can be used as a criterion for the convergence of the number of terms to be retained in the summation over l while calculating quantities such as LDOS near the surface of a sphere, like in [52]. Since the convergence criterion in Eq. (13) depends on R_2, we anticipate that the method outlined in Ref. [41] cannot be extended directly to the case of near-field radiative transfer between a sphere and a parallel surface [37].

2.2. Convergence of summation over m

In addition to truncating the infinite series in Eq. (8) and (9) with respect to l, it is also necessary to truncate the series in m. Since each value of m contributes independent of other values of m to the spectral conductance (and conductance), we can write $G_\omega = \sum_{m=0}^{\max(l)} G_\omega^{(m)}$, where $\max(l)$ is the maximum value of l used in the computation. The variation of $G_\omega^{(m)}$ with m between two spheres of radii $R = 25\,\mu$m and gap d = 250 nm at a resonant frequency ($\omega = 0.061$ eV) and a nonresonant frequency ($\omega = 0.1005$ eV) are shown in Fig. 6(a) and Fig. 6(b) respectively. We notice that there is an approximately exponential decay $[G_\omega^{(m)} \approx A\exp(-Bm)]$ in the contributions from higher values of m. The values of B for the resonant and nonresonant frequency are shown in Fig. 6(a) and Fig. 6(b) respectively. This observation enables us to propose an empirical criterion for the number of terms M_{conv} to be retained in summation over m as:

$$G_\omega^{(M_{conv})} = 0.005 G_\omega^{(0)} \tag{14}$$

#147197 - $15.00 USD Received 9 May 2011; revised 26 May 2011; accepted 27 May 2011; published 6 Jun 2011

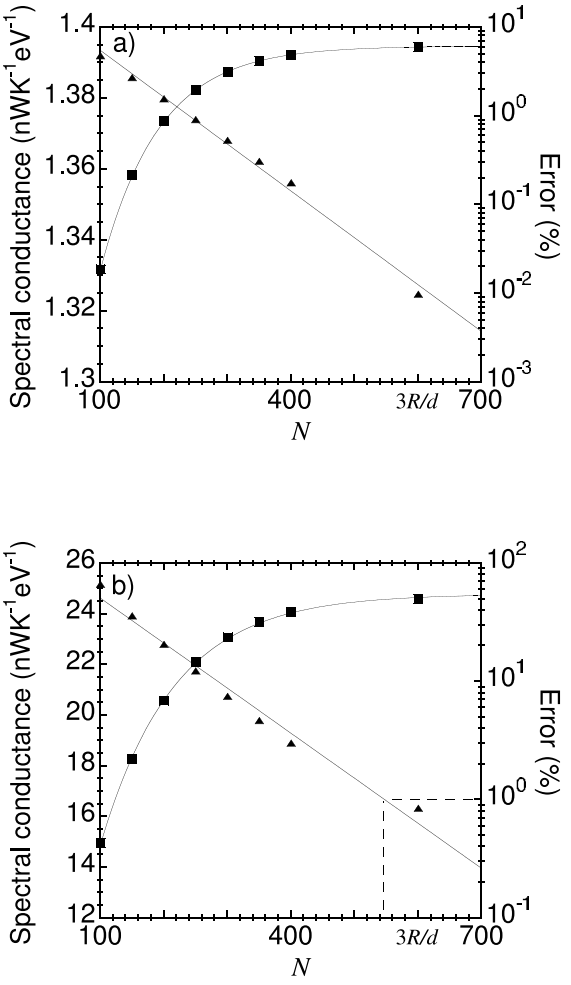

Fig. 5. Convergence of spectral conductance shown for $R_1 = 2\,\mu$m and $R_2 = 40\,\mu$m spheres for d = 200 nm at **(a)** a nonresonant frequency (0.1005 eV) **(b)** a resonant frequency (0.061 eV).

#147197 - $15.00 USD Received 9 May 2011; revised 26 May 2011; accepted 27 May 2011; published 6 Jun 2011

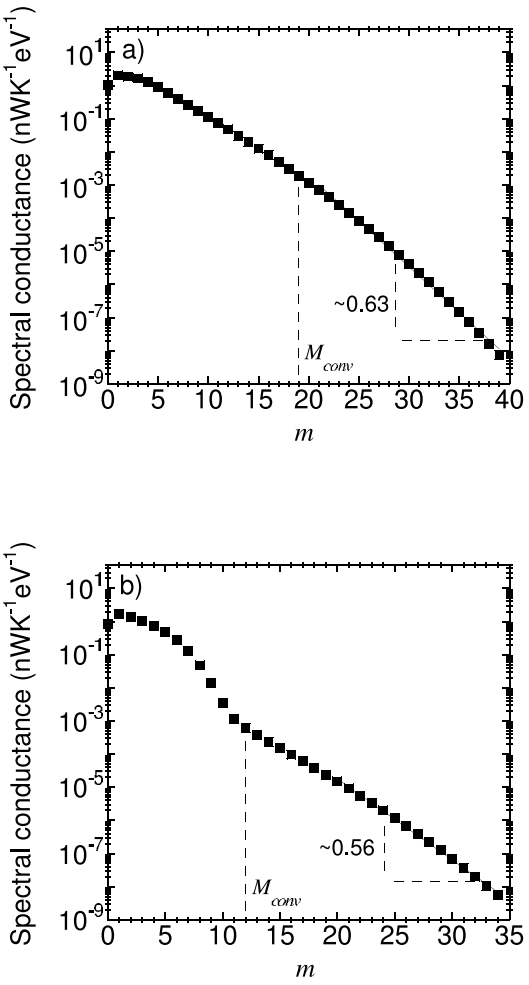

Fig. 6. Contribution to spectral conductance from each value of m for $R = 25\,\mu$m and d = 250 nm at **(a)** a resonant frequency (0.061 eV) **(b)** nonresonant frequency (0.1005 eV). The rate of exponential decay (B) for higher values of m at the resonant frequency is also shown.

#147197 - $15.00 USD Received 9 May 2011; revised 26 May 2011; accepted 27 May 2011; published 6 Jun 2011

i.e only wavefunctions with contribution to spectral conductance higher than 0.5% of the contribution from $m = 0$ are used for the series summation in m in Eq. (8) and Eq. (9). For the case considered in Fig. 6, the error due to retaining contributions only from the wavefunctions satisfying Eq. (14) is $\approx 0.028\%$ at the resonant frequency and $\approx 0.024\%$ at the nonresonant frequency.

3. Concluding remarks

To summarize, we have investigated the numerical convergence of vector spherical wave expansion technique applied to near-field electromagnetic scattering. The conclusions of this study are as follows:

1. The number of vector spherical waves required for numerical convergence of near-field radiative thermal conductance between two closely spaced spheres of equal size that support surface polaritons is given by $N_{conv} = C\frac{R}{d} + e\pi\frac{D}{\lambda}$, where C is a dimensionless number that depends on the desired accuracy. For spheres of unequal radii, R is replaced by the radius of the larger sphere.

2. Contributions from larger values of m decay exponentially with m and the summation over m can be truncated at a value of $m = M_{conv} \ll N_{conv}$.

3. The convergence criteria developed here are also applicable to other near-field scattering problems where a new length scale is introduced in lieu of d. For example, to determine the LDOS at a point at a distance $z(\ll \lambda)$ from the surface of a sphere, the convergence criterion would be $N_{conv} = C\frac{R}{z} + e\pi\frac{D}{\lambda}$.

Acknowledgments

This work is funded partially by National Science Foundation Grant CBET-0853723.

#147197 - $15.00 USD Received 9 May 2011; revised 26 May 2011; accepted 27 May 2011; published 6 Jun 2011